

# Earthworms: multiscale (generalised wavelet?) analysis of the EGM96 gravity field model of the Earth

Franklin G. Horowitz<sup>1</sup>, Peter Hornby<sup>1</sup>, Gabriel Strykowski<sup>2</sup>, Fabio Boschetti<sup>1</sup>

<sup>1</sup>CSIRO, Division of Exploration and Mining, PO Box 1130, Bentley WA 6102, Australia, (email: {frank,peterho, fabio}@ned.dem.csiro.au, phone: +61 8 6436 8500, fax: +61 8 6436 8555)

<sup>2</sup>KMS (National Survey and Cadastre), Rentermestervej 8, Copenhagen, DK-2400, Denmark, (email: gs@kms.dk, phone: +45 35 87 53 16, fax: +45 35 87 50 52)

## Abstract

We perform edge detection on the EGM96 global geodetic gravity field model, which has an approximate resolution of 30 minutes of arc over the entire Earth. The technique is in accord with our wavelet based multiscale edge analysis, which is valid for a flat earth approximation. For the spherical earth, the technique yields a one-parameter family of curves, localized with changing length scales, which differ from a classical wavelet transform. However, they share some of the desirable features of wavelets, and data analysis over the whole Earth appear as interpretable as the flat earth results at short scales.

## Introduction

In a number of previous papers, we have described the theory and applications of a wavelet based multiscale edge analysis of potential fields under a flat earth approximation. Such edges, which we colloquially call "worms", form a skeletonization of the gravity field that simultaneously has appealing theoretical properties (e.g. Hornby et al., 1999) and useful practical interpretations (e.g. Archibald et al., 1998).

In this paper we apply a similar technique to the EGM96 field (Lemoine, et al. 1997). EGM96 represents the geodetic community's best model, to 1997, of the Earth's gravitational field complete to spherical harmonic degree-and-order 360 (roughly 30 minutes of arc). For those readers uninterested in mathematical detail, an informal description of the technique along with both a movie and an interactive VRML model of the results are archived via a link near the top of <http://www.ned.dem.csiro.au/HorowitzFrank>.

## Theory

### Flat Earth

Let  $T$  be the scalar (gravitational) potential for an anomalous gravity field. Using the subscripted comma convention to denote differentiation, in a flat earth approximation  $T_{,z} = \partial T / \partial z$  might represent (e.g.) the Bouguer anomaly or the free-air anomaly, depending upon which corrections have been applied to the gravity measurements. We define multiscale edges as the positions and (scaled) magnitudes of local maxima in the modulus of the horizontal gradient of  $T_{,z}$  (i.e.  $M = \sqrt{T_{,zx}^2 + T_{,zy}^2}$  where  $x$  and  $y$  are, e.g., East and North respectively) at multiple upward continuation heights. Hornby et al. (1999; along with Moreau et al., 1997) have shown that upward continuation of  $T_{,z}$  is identical to the scale change operation for a continuous wavelet transform whose smoothing function is the scaled Green's function for  $T_{,z}$ . The (2D vector valued) wavelet transform components are  $T_{,zx}$  and  $T_{,zy}$ .

## Spherical Earth

Using spherical harmonics, we can decompose a function  $f_r(\bar{\mathbf{e}}_r)$  on the sphere of radius  $r$  as:

$$\hat{f}_r(\ell, m) = \int f_r(\bar{\mathbf{e}}_r) Y_\ell^m(\bar{\mathbf{e}}_r)^* d\bar{\mathbf{e}}_r \quad (1)$$

Here, the  $Y_\ell^m(\bar{\mathbf{e}}_r) = Y_\ell^m(\vartheta, \lambda) \equiv (-1)^m \sqrt{\frac{2\ell+1}{4\pi} \frac{(\ell-m)!}{(\ell+m)!}} P_\ell^m(\cos \vartheta) e^{im\lambda}$  are fully normalized spherical harmonics (expressed in terms of the associated Legendre function  $P_\ell^m(x)$ , the co-latitude  $\vartheta$ , and the longitude  $\lambda$  — in the conventional geodetic nomenclature),  $\bar{\mathbf{e}}_r$  is a unit vector in the  $\bar{\mathbf{r}}$  direction, and a superposed asterisk denotes complex conjugation.

It is shown in Arfken and Weber (1995; eqn 8.187) that the Green's function for Laplace's equation (with sources) expressed in spherical harmonics is given by:

$$\Gamma(\bar{\mathbf{r}}', \bar{\mathbf{r}}) = \frac{1}{4\pi} \frac{1}{|\bar{\mathbf{r}}' - \bar{\mathbf{r}}|} = \sum_{\ell=0}^{\infty} \sum_{m=-\ell}^{\ell} \frac{1}{2\ell+1} \frac{r'^{\ell}}{r^{\ell+1}} Y_\ell^m(\bar{\mathbf{e}}_r) Y_\ell^m(\bar{\mathbf{e}}_{r'})^* \quad (2)$$

Here,  $r' = |\bar{\mathbf{r}}'|$  is the radius of the point mass in the interior of the Earth, and  $r = |\bar{\mathbf{r}}|$  is the radius of the point exterior to the Earth at which we observe the effects of the point mass.

The above expression yields the potential due to a point source (to within the product of Newton's gravitational constant  $G$ , and the mass of the point source). However, we are interested in the radial derivative of the potential, i.e. the radial (vertical) acceleration due to that point mass.

$$\bar{\mathbf{g}}_r(\bar{\mathbf{r}}', \bar{\mathbf{r}}) = \frac{\partial}{\partial r} \Gamma(\bar{\mathbf{r}}', \bar{\mathbf{r}}) = \bar{\mathbf{e}}_r \sum_{\ell=0}^{\infty} \sum_{m=-\ell}^{\ell} \frac{-(\ell+1)}{2\ell+1} \frac{r'^{\ell}}{r^{\ell+2}} Y_\ell^m(\bar{\mathbf{e}}_r) Y_\ell^m(\bar{\mathbf{e}}_{r'})^* \quad (3)$$

Given the above background, we write for a vertical (radial) magnitude of gravity field on the sphere:

$$\begin{aligned} f(\bar{\mathbf{r}}) &= f_r(\bar{\mathbf{e}}_r) = f(r\bar{\mathbf{e}}_r) \\ &= -\frac{G}{4\pi} \int \frac{\partial}{\partial r} \left( \frac{1}{\|\bar{\mathbf{r}} - \bar{\mathbf{r}}'\|} \right) \rho(\bar{\mathbf{r}}') d\bar{\mathbf{r}}' \\ &= -\frac{G}{4\pi} \int \frac{\partial}{\partial r} \left( \frac{1}{\|\bar{\mathbf{r}} - \bar{\mathbf{r}}'\|} \right) \rho(\bar{\mathbf{r}}') r'^2 dr' d\bar{\mathbf{e}}_{r'} \\ &= G \int_0^{r_0} dr' r'^2 \int \sum_{\ell, m} \frac{\ell+1}{2\ell+1} \frac{r'^{\ell}}{r^{\ell+2}} Y_\ell^m(\bar{\mathbf{e}}_r) Y_\ell^m(\bar{\mathbf{e}}_{r'})^* \rho_{r'}(\bar{\mathbf{e}}_{r'}) d\bar{\mathbf{e}}_{r'} \\ &= G \int_0^{r_0} dr' \int d\bar{\mathbf{e}}_{r'} \sum_{\ell, m} \frac{\ell+1}{2\ell+1} \frac{r'^{\ell+2}}{r^{\ell+2}} Y_\ell^m(\bar{\mathbf{e}}_r) Y_\ell^m(\bar{\mathbf{e}}_{r'})^* \rho_{r'}(\bar{\mathbf{e}}_{r'}) \\ &= G \int_0^{r_0} dr' \sum_{\ell, m} \left( \frac{r'}{r} \right)^{\ell+2} \frac{\ell+1}{2\ell+1} Y_\ell^m(\bar{\mathbf{e}}_r) \hat{\rho}_{r'}(\ell, m) \end{aligned} \quad (4)$$

Hence, we find for  $f(\bar{\mathbf{r}})$  expressed in spherical harmonics:

$$\hat{f}_r(\ell, m) = G \int d\bar{\mathbf{e}}_r \sum_{\ell', m'} \int_0^{r_0} dr' \hat{\rho}_{r'}(\ell', m') \left( \frac{r'}{r} \right)^{\ell+2} \frac{\ell+1}{2\ell+1} Y_{\ell'}^{m'}(\bar{\mathbf{e}}_r) Y_\ell^m(\bar{\mathbf{e}}_r)^* \quad (5)$$

but we use orthonormalised  $Y_\ell^m$  so that

$$\int d\bar{\mathbf{e}}_r Y_{\ell'}^{m'}(\bar{\mathbf{e}}_r) Y_\ell^m(\bar{\mathbf{e}}_r) = \delta_{\ell', \ell} \delta_{m', m} \quad (6)$$

which leads to

$$\hat{f}_r(\ell, m) = G \frac{\ell+1}{2\ell+1} \left( \frac{1}{r} \right)^{\ell+2} \int_0^{r_0} \hat{\rho}_{r'}(\ell, m) r'^{\ell+2} dr' \quad (7)$$

We now derive a method for taking a field expressed at one height to its upward (outward)

continuation at another height. Denoting the integral in Equation (7) by  $I_{\ell+2}[\hat{\rho}_{r'}](\ell, m)$ , we find

$$\hat{f}_r(\ell, m) = G \frac{\ell+1}{2\ell+1} \left(\frac{1}{r}\right)^{\ell+2} I_{\ell+2}[\hat{\rho}_{r'}](\ell, m) \quad (8)$$

which leads to

$$\hat{f}_{r_0}(\ell, m) = G \frac{\ell+1}{2\ell+1} \left(\frac{1}{r_0}\right)^{\ell+2} I_{\ell+2}[\hat{\rho}_{r'}](\ell, m) \quad (9)$$

hence

$$\hat{f}_r(\ell, m) = \left(\frac{r_0}{r}\right)^{\ell+2} \hat{f}_{r_0}(\ell, m) \quad (10)$$

and so, the transfer function taking the spherical harmonic field from level  $r_0$  to level  $r$  is given by

$$\hat{\gamma}_{r_0, r} = \left(\frac{r_0}{r}\right)^{\ell+2} \quad (11)$$

Back transforming the two transform variables from the spherical harmonic domain to the spatial domain, we write:

$$\gamma(\bar{\mathbf{r}}, \bar{\mathbf{r}}_0) = \sum_{\ell, m} \left(\frac{r_0}{r}\right)^{\ell+2} Y_{\ell}^m(\bar{\mathbf{e}}_r) Y_{\ell}^m(\bar{\mathbf{e}}_{r_0})^* \quad (12)$$

Now, with the preceding as background we begin to build a “wavelet-like” construct, in analog with our flat earth case. We start by writing our “smoothing function at the origin” as being due to a point mass source at the North Pole (at Earth radius  $r_0$ ):

$$\gamma(\bar{\mathbf{r}}, r_0 \bar{\mathbf{e}}_z) = \sum_{\ell, m} \left(\frac{r_0}{r}\right)^{\ell+2} Y_{\ell}^m(\bar{\mathbf{e}}_r) Y_{\ell}^m(\bar{\mathbf{e}}_z)^* \quad (13)$$

Now, since we have fixed one of the angular freedoms to be aligned with the  $z$ -axis, Equation (13) is really a function of one angular variable. Hence, we define a new function, which takes the field due to a point source at the North Pole to radius  $r_1 > r_0$ :

$$\Theta(\bar{\mathbf{e}}_{r_1}) = \gamma(\bar{\mathbf{r}}_1, r_0 \bar{\mathbf{e}}_z) = \sum_{\ell, m} \left(\frac{r_0}{r_1}\right)^{\ell+2} Y_{\ell}^m(\bar{\mathbf{e}}_r) Y_{\ell}^m(\bar{\mathbf{e}}_z)^* \quad (14)$$

Integrating  $\Theta$  over the sphere, and making use of Equation (6) with the fact that  $Y_0^0 = 1/\sqrt{4\pi}$ , a constant (Arfken and Weber, 1995, Table 12.3), we find:

$$\int \Theta(\bar{\mathbf{e}}') d\bar{\mathbf{e}}' = \int d\bar{\mathbf{e}}' \frac{1}{\sqrt{4\pi}} \left(\frac{r_0}{r_1}\right)^2 Y_0^0(\bar{\mathbf{e}}_z)^* = \left(\frac{r_0}{r_1}\right)^2 \quad (15)$$

Normalizing our smoothing function with this factor allows us to define a new unit weight smoothing function:

$$\theta(\bar{\mathbf{e}}) = \left(\frac{r_1}{r_0}\right)^2 \sum_{\ell, m} \left(\frac{r_0}{r_1}\right)^{\ell+2} Y_{\ell}^m(\bar{\mathbf{e}}) Y_{\ell}^m(\bar{\mathbf{e}}_z)^* = \left(\frac{r_1}{r_0}\right)^2 \Theta(\bar{\mathbf{e}}) \quad (16)$$

From this, we see that

$$\theta(\bar{\mathbf{e}}) = \sum_{\ell, m} \left(\frac{r_0}{r_1}\right)^{\ell} Y_{\ell}^m(\bar{\mathbf{e}}) Y_{\ell}^m(\bar{\mathbf{e}}_z)^* \quad (17)$$

or

$$\hat{\theta}(\ell, m) = \left(\frac{r_0}{r_1}\right)^{\ell} Y_{\ell}^m(\bar{\mathbf{e}}_z)^* \text{ and } \int \theta(\bar{\mathbf{e}}) d\bar{\mathbf{e}} = 1 \quad (18)$$

If we define  $\phi_r(\bar{\mathbf{e}}) = (r/r_0)^2 \gamma(\bar{\mathbf{r}}, r_0 \bar{\mathbf{e}}_z)$  for some new height  $r > r_1 > r_0$ , we find  $\int \phi_r(\bar{\mathbf{e}}) d\bar{\mathbf{e}} = 1$ .

Now,

$$\hat{\phi}_r = \left(\frac{r_0}{r}\right)^\ell Y_\ell^m(\bar{\mathbf{e}}_z)^* = \left(\frac{r_0}{r_1}\right)^\ell \left(\frac{r_1}{r}\right)^\ell Y_\ell^m(\bar{\mathbf{e}}_z)^* = \left(\frac{r_1}{r}\right)^\ell \hat{\theta}(\ell, m) \quad (19)$$

and

$$\begin{aligned} f_r(\bar{\mathbf{e}}_r) &= \int \gamma(\bar{\mathbf{r}}, r_0 \bar{\mathbf{e}}_z) f_{r_0}(\bar{\mathbf{e}}_{r_0}) d\bar{\mathbf{e}}_{r_0} \\ &= \int \gamma(\bar{\mathbf{r}}, r_0 \Omega(\bar{\mathbf{e}}_z \rightarrow \bar{\mathbf{e}}_{r_0}) \bar{\mathbf{e}}_z) f_{r_0}(\bar{\mathbf{e}}_{r_0}) d\bar{\mathbf{e}}_{r_0} \\ &= \int \gamma(\Omega^T(\bar{\mathbf{e}}_z \rightarrow \bar{\mathbf{e}}_{r_0}) \bar{\mathbf{r}}, r_0 \bar{\mathbf{e}}_z) f_{r_0}(\bar{\mathbf{e}}_{r_0}) d\bar{\mathbf{e}}_{r_0} \\ &= \left(\frac{r_0}{r}\right)^2 \int \phi_r(\Omega^T(\bar{\mathbf{e}}_z \rightarrow \bar{\mathbf{e}}_{r_0}) \bar{\mathbf{r}}) f_{r_0}(\bar{\mathbf{e}}_{r_0}) d\bar{\mathbf{e}}_{r_0} \end{aligned} \quad (20)$$

where  $\Omega$  is a rotation operator. In other words, we see that the following two convolution relations, re-scaled for the two different heights, hold:

$$\phi_r * f_{r_0} = \left(\frac{r}{r_0}\right)^2 f_r(\bar{\mathbf{e}}_r) \quad (21)$$

and

$$\theta * f_{r_0} = \left(\frac{r_1}{r_0}\right)^2 f_{r_1}(\bar{\mathbf{e}}_{r_1}) \quad (22)$$

But, we know that

$$\theta(\bar{\mathbf{e}}) = \sum_{\ell, m} \left(\frac{r_0}{r_1}\right)^\ell Y_\ell^m(\bar{\mathbf{e}}) Y_\ell^m(\bar{\mathbf{e}}_z)^* \quad (23)$$

and

$$\phi_r(\bar{\mathbf{e}}) = \sum_{\ell, m} \left(\frac{r_0}{r}\right)^\ell Y_\ell^m(\bar{\mathbf{e}}) Y_\ell^m(\bar{\mathbf{e}}_z)^* \quad (24)$$

From this, we conclude that the  $(\ell, m)$  components of  $\theta(\bar{\mathbf{e}})$  and  $\phi_r(\bar{\mathbf{e}})$  are (respectively):

$$\hat{\theta} = \left(\frac{r_0}{r_1}\right)^\ell Y_\ell^m(\bar{\mathbf{e}}_z)^* \quad (25)$$

$$\hat{\phi}_r = \left(\frac{r_0}{r}\right)^\ell Y_\ell^m(\bar{\mathbf{e}}_z)^* = \left(\frac{r_1}{r}\right)^\ell \left(\frac{r_0}{r_1}\right)^\ell Y_\ell^m(\bar{\mathbf{e}}_z)^* \quad (26)$$

This finally brings us to the result:

$$\hat{\phi}_r = \left(\frac{r_1}{r}\right)^\ell \hat{\theta} \quad (27)$$

Equation (27) shows the spherical harmonic domain outward continuation operator between a field represented at two heights. This is the analog of the well-known flat earth case Fourier domain upward continuation operator:  $\exp(-2\pi i \|\mathbf{k}\| |\Delta z|)$ .

### Wavelet scaling on the sphere

Because great circle/geodesic arc-length on the surface of a sphere is proportional to radius, the radius itself is a natural scaling parameter for a sphere. Since the spherical harmonic functions themselves are defined only in terms of angular variables ( $\bar{\mathbf{e}}_r$ , or equivalently  $\vartheta$  and  $\lambda$ ), ‘‘inflating’’ them to maintain their shape at different radii yields expressions that are independent of radius. However, as can be seen from Equation (27), outward continuation in

the spherical harmonic domain contains a different power of the radius ratio for each degree,  $\ell$ . Hence, the smoothing function does not maintain its shape with outward continuation.

This brings us to the central result of this paper: *Laplace/Poisson's equation on a sphere does not yield the traditional style of space-stretching wavelet scaling that Laplace/Poisson's equation in the plane does* (e.g. Hornby et al, 1999). This means that we cannot use any of the results from traditional wavelet theory without proving applicability to the present case. Obviously, this is a large task. Clearly, we have a wavelet in the limiting flat earth case. Indeed, the flat earth approximation can be thought of as the case where  $r_1$  is "close enough" to  $r$  such that their ratio is "effectively" 1, and hence its power in Equation (27) is "effectively" 1 for all "interesting" values of  $\ell$ .

We believe that not all is lost, however. We motivate this belief by graphing our Poissonian smoother, and its derivative as the candidate "generalized wavelet". In order to accomplish this, we first need a few auxiliary manipulations. Central to our construction is the radial acceleration field due to a point mass source at the North Pole. Since we have chosen to place the mass at the North Pole (ignoring hemispherical chauvinism), then by symmetry, the Green's function cannot be a function of longitude (i.e. all  $m \neq 0$  terms drop out):

$$\begin{aligned}
\theta(\vec{\mathbf{e}}) &= \sum_{\ell,m} \left( \frac{r_0}{r_1} \right)^\ell Y_\ell^m(\vec{\mathbf{e}}) Y_\ell^m(\vec{\mathbf{e}}_z)^* \\
&= \sum_{\ell} \left( \frac{r_0}{r_1} \right)^\ell Y_\ell^0(\vec{\mathbf{e}}) Y_\ell^0(\vec{\mathbf{e}}_z)^* \\
&= \sum_{\ell} \left( \frac{r_0}{r_1} \right)^\ell \sqrt{\frac{2\ell+1}{4\pi}} \sqrt{\frac{2\ell+1}{4\pi}} P_\ell(\cos \vartheta) P_\ell(\cos 0) \\
&= \frac{1}{4\pi} \sum_{\ell} \left( \frac{r_0}{r_1} \right)^\ell (2\ell+1) P_\ell(\cos \vartheta)
\end{aligned} \tag{28}$$

Here, we have made use of the definition of associated Legendre functions  $P_\ell^m(x) = (1-x^2)^{m/2} \frac{d^m}{dx^m} P_\ell(x)$ , with the  $P_\ell(x)$  being Legendre polynomials, and the (easily verified) property  $P_\ell(1) = 1 \quad \forall \ell \geq 0$  (e.g., see Arfken and Weber, 1995, equation 12.81, and table 12.1 or recurrence relation 12.17). We normalize by  $\theta(\vec{\mathbf{e}}_z)$  as follows:

$$\theta(\vec{\mathbf{e}}_z) = \sum_{\ell,m} \left( \frac{r_0}{r_1} \right)^\ell Y_\ell^m(\vec{\mathbf{e}}_z) Y_\ell^m(\vec{\mathbf{e}}_z)^* \tag{29}$$

but, again by symmetry, the  $Y_\ell^m$  terms drop out for  $m \neq 0$ , leading to

$$\begin{aligned}
\theta(\bar{\mathbf{e}}_z) &= \sum_{\ell} \left( \frac{r_0}{r_1} \right)^{\ell} \left| Y_{\ell}^0(\bar{\mathbf{e}}_z) \right|^2 \\
&= \sum_{\ell} \left( \frac{r_0}{r_1} \right)^{\ell} \frac{(2\ell+1)P_{\ell}(1)}{4\pi} \\
&= \frac{1}{4\pi} \sum_{\ell} (2\ell+1) \left( \frac{r_0}{r_1} \right)^{\ell} \\
&= \frac{1}{4\pi} \frac{\left( 1 + \frac{r_0}{r_1} \right)}{\left( 1 - \frac{r_0}{r_1} \right)^2} \\
&= \frac{1}{4\pi} \frac{r_1(r_1+r_0)}{(r_1-r_0)^2}
\end{aligned} \tag{30}$$

Notice how dividing by Equation (30) yields a physically relevant scaling, with  $r_0$  playing a central role. When  $r_1 = r_0$ , we find a natural definition of scale 0. When  $r_1 = \infty$ , we find a natural definition of scale +1. Finally, when  $r_1 = 0$ , we find a natural definition of scale  $-\infty$  (perhaps implying that negative scales are appropriate for the so-called “inner” spherical harmonic expansion of geodesy). We plot Equation (28) normalized by Equation (30) in Figure 1.

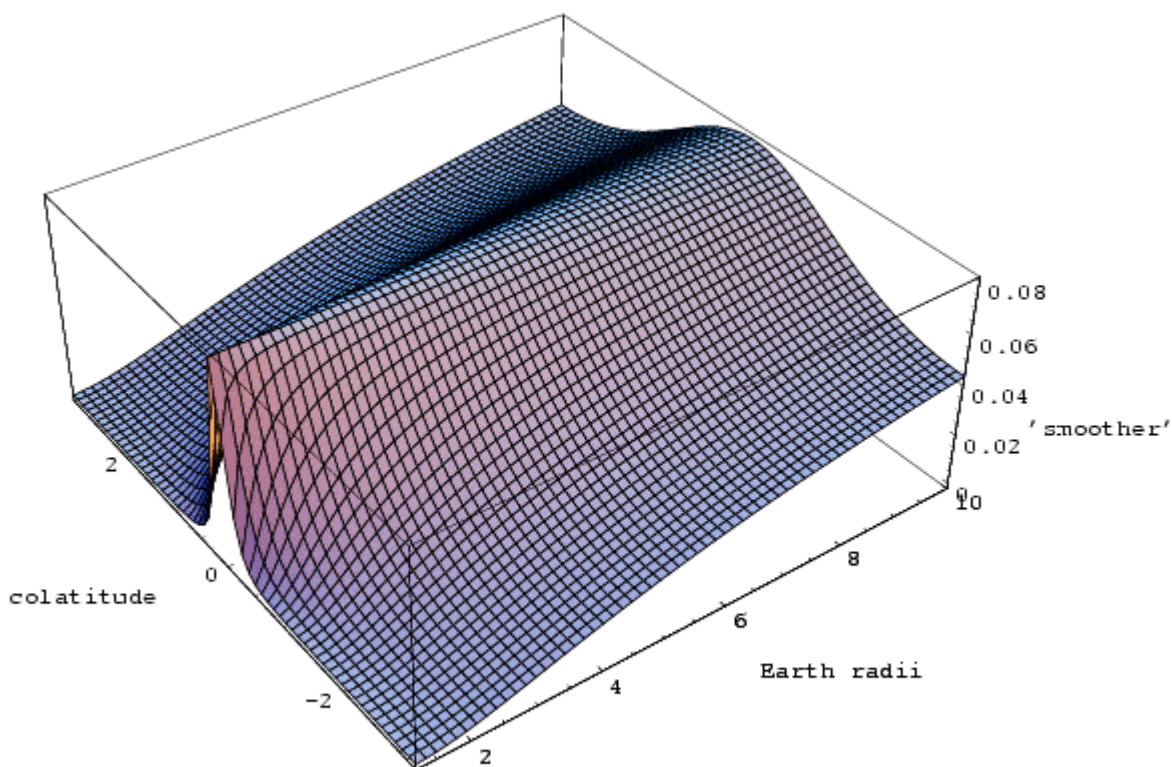


Figure 1. The “wavelet” smoothing/scaling function of Equation (28), graphed with  $\ell$  summed from 0 through 50 for a suite of different heights. Colatitude ( $\vartheta$ ) is given in radians, with 0 representing the North Pole, and the function being rotationally symmetric about the

“epicentral” point. Although the function numerically starts to misbehave for radii approaching 1, it is in fact a delta function, as can be inferred from Equation (6). The rotationally symmetric function is convolved with the radial gravity field at radius=1, yielding the upward (outward) continued version of the field.

The preceding is our candidate “generalized wavelet smoothing/scaling” function. To define our candidate wavelet, we differentiate Equation (28) with respect to colatitude:

$$\begin{aligned}
 \frac{d\theta}{d\vartheta} &= \frac{-1}{4\pi} \sum_{\ell} \left(\frac{r_0}{r_1}\right)^{\ell} (2\ell+1) \sin \vartheta P'_{\ell}(\cos \vartheta) \\
 &= \frac{-\sin \vartheta}{4\pi} \sum_{\ell} \left(\frac{r_0}{r_1}\right)^{\ell} (2\ell+1) \frac{\ell P_{\ell-1}(\cos \vartheta) - \ell \cos \vartheta P_{\ell}(\cos \vartheta)}{\sin^2 \vartheta} \\
 &= \frac{+1}{4\pi \sin \vartheta} \sum_{\ell} \left(\frac{r_0}{r_1}\right)^{\ell} \ell(2\ell+1) [\cos \vartheta P_{\ell}(\cos \vartheta) - P_{\ell-1}(\cos \vartheta)]
 \end{aligned} \tag{31}$$

We plot Equation (31) normalized by Equation (30) in Figure 2.

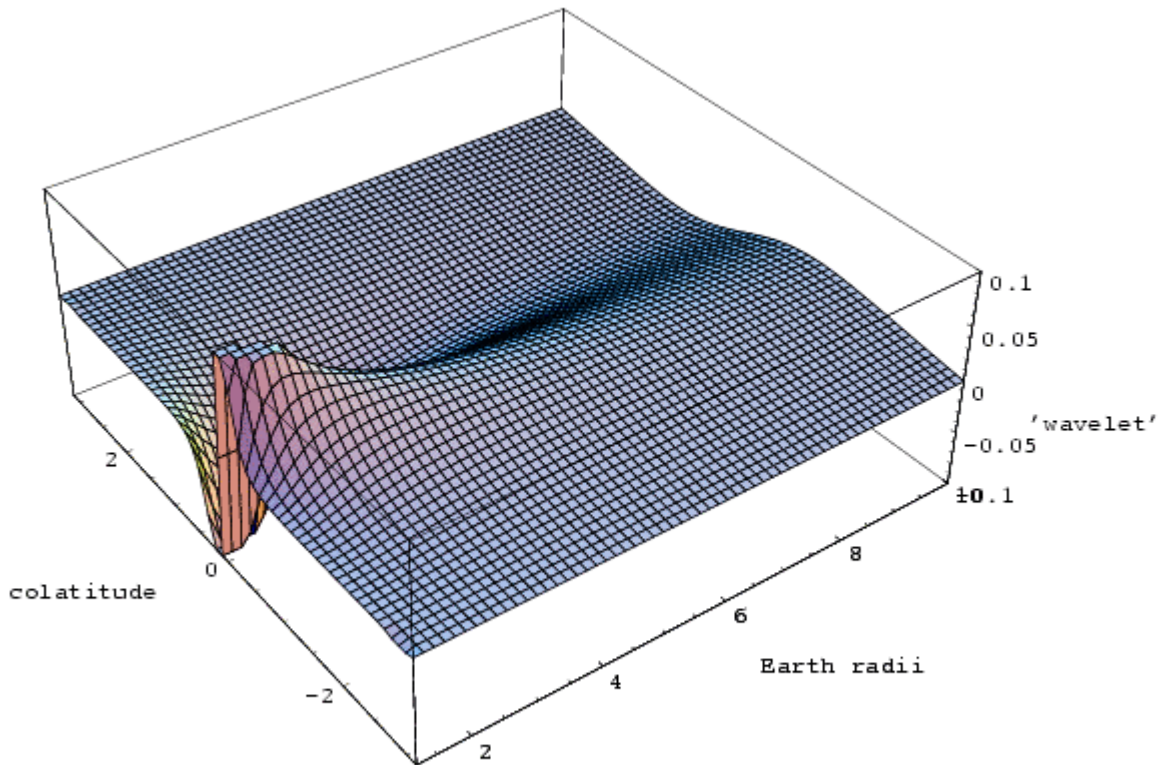


Figure 2. The “wavelet” function of Equation (31), graphed with  $\ell$  summed from 0 through 50 for a suite of different heights. Colatitude ( $\vartheta$ ) is given in radians, with 0 representing the North Pole. Unlike the smoother/scalar of Figure 1, this function is not rotationally symmetric. Hence when we convolve it around the sphere, orientation is significant, and the result is vector valued.

As is well known, the tangential gradient implicit in this function can be expressed in terms of spherical harmonics using the so-called “angular momentum” operator ( $\mathbf{L}$ ) of wave mechanics (exercise 12.6.7 in Arfken and Weber, 1995).

## Discussion

This analysis is not yet complete. While we have constructed a one-parameter family of functions that spatially localize signal properties of different length scales, because they do not maintain their shape with rescaling they are not wavelets in the classical sense of the term. It remains to be demonstrated whether our construction has properties that are *as useful as* classical wavelets. In future work, we hope to be able to demonstrate such properties as: allowing the estimation of Lipschitz exponents of rock discontinuities using the ideas of Mallet and Zhong (1992), or the signal processing operations via reconstruction from multiscale edges available to classical wavelets. However, for the time being, we stop the theoretical development here.

## Data analysis

On the sphere, by analogy with the flat earth case, we define a multiscale edge to be the locus of points where the magnitude of tangential gradient vectors due to Equation (31) go through maxima. We have previously described this work in Horowitz et al., (2000a) and Horowitz et al. (2000b). In fact, when we calculated the results displayed below (and on the website pointed to by <http://www.ned.dem.csiro.au/HorowitzFrank>) we approximated tangential derivatives not with the  $L$  operator described above, but by finite-difference calculation on an equiangular latitude-longitude grid. As such, the numerical results could be improved. Nevertheless, the visual correlation between the flat earth results we calculate for Australia and with the spherical results over the same region, lead us to believe that we have not committed too much violence with our numerical approximations.

A quick summary view is shown in Figure 3. Because of the limitations of the printing process of the conference volume, the grayscale paper version will not be too spectacular. The color figures found in the PDF version of this document, along with the online VRML versions found under the above website will undoubtedly be more informative.



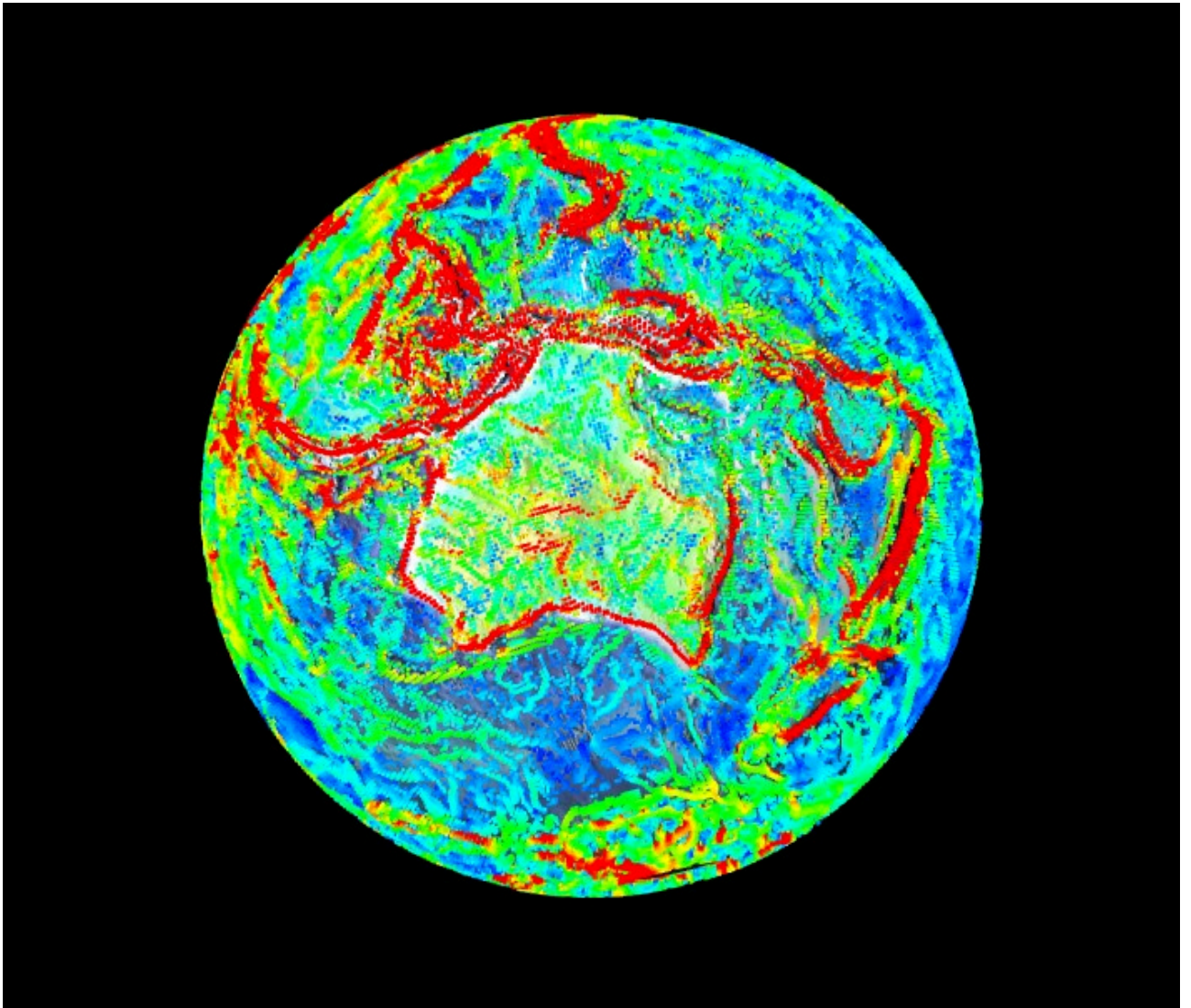


Figure 3. Earthworms over Australia at relatively low values of outward continuations.

## Summary

We have presented the spherical harmonic version of the theory behind our multiscale edge analysis of potential fields. While the result is not a wavelet in the classical sense of the word, if (with future work) we can demonstrate certain properties hold, the result on the sphere should be as useful as the flat earth results have proven themselves to be. If so, we can perhaps justify calling our construction a “generalized wavelet” for the sphere.

## References

- [1] Archibald, N.J., P. Gow, and F. Boschetti, 1998 *Multiscale edge analysis of potential field data*, Exploration Geophysics, 30, 38-44, 1998.
- [2] Arfken, G.B., and H.J. Weber, 1995 *Mathematical methods for Physicists*, Academic Press.
- [3] Hornby, P., F. Boschetti, and F.G. Horowitz, 1999 *Analysis of Potential Field Data in the Wavelet Domain*, Geophysical Journal International, 137, pp. 175-196.
- [4] Horowitz, F.G., G. Strykowski, F. Boschetti, P. Hornby, N. Archibald, D. Holden, P. Ketelaar, and R. Woodcock, 2000 *Earthworms; 'Multiscale' Edges in the EGM96 Global Gravity Field*, 70th Ann. Internat. Mtg: Soc. Of Expl. Geophys. Session: G&M 3.2, Calgary, Alberta, Canada.

- [5] Horowitz, F.G., G. Strykowski, P. Hornby, F. Boschetti, and S.J.D. Cox, 2000 *A Multiscale Skeletonization of the EGM96 Gravity Disturbances, Locally Compared with Australian Geophysical Data*, poster 2.3 at the IAG International Symposium on Gravity, Geoid and Geodynamics 2000, Banff, Alberta, Canada.
- [6] Lemoine, F. G., D. E. Smith, L. Kunz, R. Smith, E. C. Pavlis, N. K. Pavlis, S. M. Klosko, D. S. Chinn, M. H. Torrence, R. G. Williamson, C. M. Cox, K. E. Rachlin, Y. M. Wang, S. C. Kenyon, R. Salman, R. Trimmer, H. R. Rapp, and R. S. Nerem, 1997 *The Development of the NASA GSFC and NIMA Joint Geopotential Model*, in: Gravity, Geoid and Marine Geodesy, Vol. 117, International Association of Geodesy Symposia, J. Segawa, H. Fujimoto, and S. Okubo (editors), pp 461-469.
- [7] Mallat, S., and S. Zhong, 1992 *Characterisation of signals from multiscale edges*, IEEE Transactions on Pattern Analysis and Machine Intelligence, 14, 710-32.
- [8] Moreau, F., D. Gilbert, M. Holshneider, and D. Saracco, 1997 *Wavelet analysis of potential fields*, Inverse Problems, 13, 165-178.